

# CAMERA CALIBRATION IN A HAZARDOUS ENVIRONMENT PERFORMED IN SITU WITH AUTOMATED ANALYSIS AND VERIFICATION\*

Frederick W. DePiero  
Robotics & Process Systems Division  
Oak Ridge National Laboratory  
P.O. Box 2008, Bldg. 7601  
Oak Ridge, Tennessee 37831-6304  
Telephone 615-574-8951  
Facsimile 615-576-2081

Reid L. Kress  
Robotics & Process Systems Division  
Oak Ridge National Laboratory  
P.O. Box 2008, Bldg. 7601  
Oak Ridge, Tennessee 37831-6304  
Telephone 615-574-2468  
Facsimile 615-576-2081

**ABSTRACT** Camera calibration using the method of Two Planes is discussed. An implementation of the technique is described that may be performed in situ, e.g., in a hazardous or contaminated environment, thus eliminating the need for decontamination of camera systems before recalibration. Companion analysis techniques useful for verifying the correctness of the calibration are presented.

## INTRODUCTION

The potential for risk to operators is high when hazardous waste generated from environmental restoration and waste management activities is handled and processed. There exist two current options to alleviate the hazard to operators. Operators can dress in Class "C" fully encapsulated suits, or they can process the material in a containment system. The cost of using operators in encapsulated suits is prohibitive; therefore, this option is suitable only for nonroutine operations or situations where containment systems are impractical. Encapsulated suits are often used for waste-site characterization, emergencies involving hazardous materials, and nonroutine maintenance. Operation in a containment system is the most cost-effective and safe option; thus, the Waste Processing Operations area of the Office of Technology Development, Robotics Technology Development Program is focusing on the development of remote automated systems for chemical and physical processing of waste materials. The goal is to improve productivity, reduce wastes, and minimize operator hazards.

The development of a general purpose automated glovebox containment system for processing of mixed wastes is justified based on assessment of the conditions expected in waste facilities (e.g., in the processing of radioactive wastes in the Mixed Waste Treatment Project). An appropriate and immediate application of automated glovebox containment systems is in the development of automated metal purification technology for metal recycling and reuse. This technology will require the development of automated handling and cleaning techniques for metals and for integrated operation of purification equipment. These new techniques will lead to reuse and recycling systems for lead, stainless steels, mild steel, and other alloys. The technology is expected to reduce the amount of final waste for disposal. In particular, process flow diagrams show a major lead waste stream of 6800 kg/week. This equates to the processing of 1.5 tons of lead per day in a controlled setting; therefore, attention to the development of an automated glovebox containment system for the processing of lead waste is a task of current interest.

Currently, three subtasks support the development of an automated glovebox containment system: the integration of a new IBM controller with the IBM manipulator mechanical and electrical systems already installed in a glovebox testbed at Lawrence Livermore National Laboratory, the integration of interactive control technologies with the new controller, and the development and integration of an object-scanning system. Researchers at Oak Ridge National Laboratory (ORNL) have developed the Surface Characterization and Object Pose Equipment (SCOPE) in support of the object scanning system subtask. SCOPE uses the method of structured lighting (S. W. Holland, L. Rossol, and M. R. Ward, 1978) to measure surface roughness and to determine an object's position and orientation.

---

\*Research sponsored by the Office of Technology Development, U.S. Department of Energy, and managed by Martin Marietta Energy Systems, Inc., under contract DE-AC05-84OR21400

This paper describes an in situ camera calibration technique and two companion analysis techniques for verifying the camera model. The in situ calibration and

analyses are useful mechanisms for applications involving hazardous materials via the elimination of the need for decontamination prior to recalibration. These efforts represent a portion of the first developmental phase of SCOPE.

### CAMERA CALIBRATION

The purpose of camera calibration (K. S. Fu, et al., 1987) is to determine the precise direction of incoming illumination associated with each image pixel. The result of such a calibration is a model of the perspective effects and the distortions introduced by the camera. A description of the camera model, its use, and the calibration process follows.

Many factors affect the camera model, lens distortion is the most significant (G-Q. Wei, and S. De Ma, 1991). Other effects arise from the lack of a precise alignment between the camera's image array and the optical axis. The geometry relating the camera mount to the image array must also be modeled. Another effect

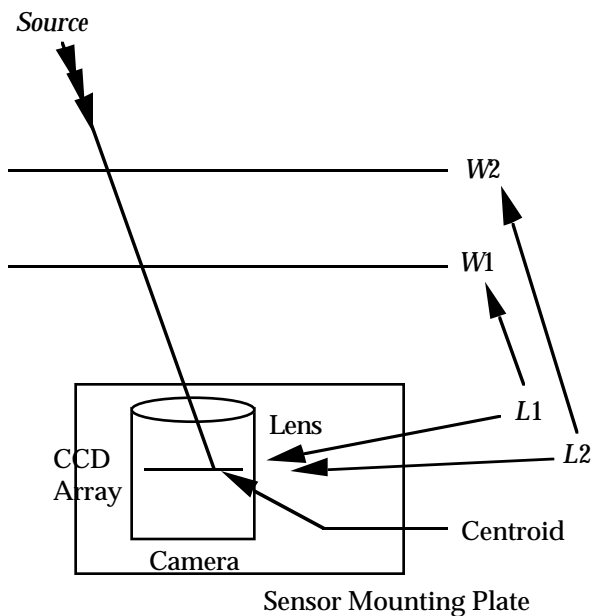


**Fig. 1. Method of Two Planes for camera calibration.** *L1* and *L2* are the camera models relating calibration planes *W1* and *W2* to pixels in the *CCD Array*. *Source* is an illumination source. *Centroid* is the pixel in the *CCD Array* corresponding to the center of the image of *Source*.

necessitating camera calibration occurs during the digitization process of an image. The synchronization of a camera with a video-to-digital converter tends to vary somewhat with individual components. Video synchronization affects the horizontal position of an

image. The effects of all these factors are modeled during the camera-calibration procedure. Hence, because the changeout of many different components can affect camera calibration, the in situ approach presented herein reduces downtime of the SCOPE sensor.

The method of Two Planes has been used to find the camera model (A. Isaguirre, P. Pu, and J. Summer, 1985). This technique proved to be very effective in recent surface mapping done at ORNL (B. L. Burks, et al. 1991; B. L. Burks, et al., 1992; B. K. P. Horn, 1984). Technique establishes the relationship between image coordinates and the three-dimensional world coordinates of a calibration target. This relationship is referred to as a camera model, and a minimum of two such models are required for two distinct targets. Once the models have been found, the direction to an illumination source can be determined. Figure 1 describes the use of the camera models. *Source* is an illumination source at some unknown distance away from the camera. The direction to *Source* is described by using points on the planes *W1* and *W2*. The direction to the source is found by first determining the image coordinate corresponding to the center of *Source's* illumination pattern. This point is labeled *Centroid* in Fig. 1. Having isolated this point of interest in the image, the camera models *L1* and *L2* are then used to map the image coordinate onto each of the two planes. Note, as Fig. 1 shows, the actual source of illumination is not located on either calibration plane.

Figure 2 shows that points along the sighting vector *F* can be represented in parametric form by

$$F = S1 + tS, \tag{1}$$

where *t* is an arbitrary scalar. The position of *F* is with respect to the camera frame *C* because the points on planes *W1* and *W2* are defined with respect to the *C*. This representation of points along the sighting vector is very useful for the ranging calculations that are required when using structured light. Here, three-dimensional range points are found by solving for the intersection of a sighting vector with a plane of laser illumination.

An attractive feature of the method of Two Planes is the ability to calibrate a camera over a wide range of distances. This is achieved by using multiple calibration planes *W1* to *Wn*. The planes are located at a variety of standoff distances from the camera which span the needed range. When measurements are required at a particular distance, the two planes closest to this range may then be used. This method tends to reduce errors that would otherwise propagate when a sighting vector is extended well beyond its point of origin.

The first step in finding the camera models is to locate a calibration target at known positions with respect to the camera. To date, a mylar sheet with dark circles

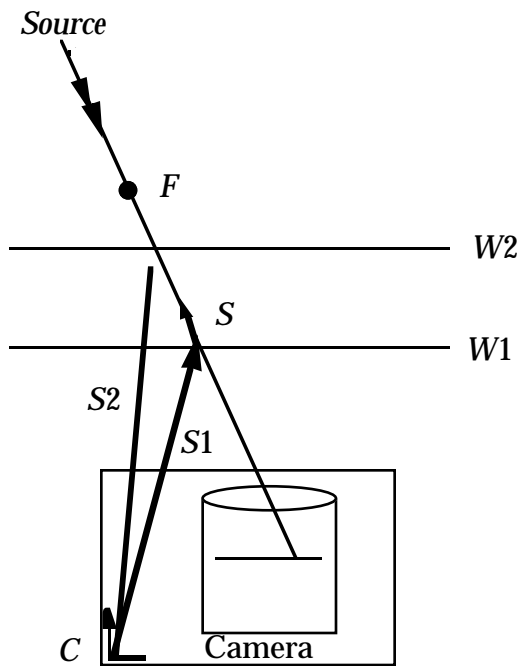


**Fig. 2. Sighting vector determination.** *C* is the reference frame attached to the camera. *S* is a vector in the direction of the illumination source. *S1* and *S2* are points of intersection between planes *W1* and *W2*, respectively, and the ray of illumination from *Source*. *F* is an arbitrary point along the sighting vector.

has been used for the calibration target along with coarse positioning equipment to locate the camera. This proved to be effective for developing the calibration and analysis software. Camera calibration in the final version of SCOPE will be accomplished in situ. The calibration procedure will consist of placing the SCOPE sensor platform onto precision mounts on a calibration jig. The jig will contain a calibration target made from optical breadboard. The breadboard will be illuminated from below and will be outfitted with a translucent platform sheet on its top surface. Its location with respect to the sensor platform will be adjustable using precision offsets. This arrangement will provide a grid of light spots at precisely known locations. Figure 3 describes the major components of the calibration jig.

The second step in finding a camera model is to capture an image of the calibration target and then to determine the image coordinate of the centroid of each light spot (or circle) seen on the target. Because of the slight flicker that is often present in lighting equipment and because of random variations in the pixel intensity of digitized images (B. K. P. Horn, 1984), multiple images were captured and averaged. Each light spot is segmented in the image by forming a binary image and then

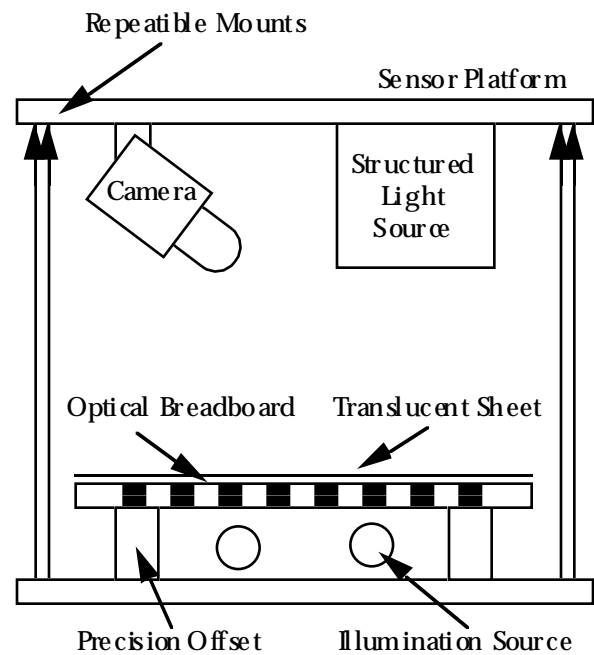


**Fig. 3. Components of the camera calibration jig.**

performing a connected component analysis (B. K. P. Horn, 1984). Once each light spot has been isolated, the centroids are found using a gray-scale weighting. This procedure involves first finding typical gray-level values in the interior of each light spot and in the background. A truncated error function is then defined that maps gray-scale values to the probability of a pixel belonging to a light spot. The error function is found by numerically integrating a Gaussian function that had been defined such that the typical background and typical light spot gray levels are three standard deviations away from the mean. This yields ~99% confidence in membership for these typical values. By performing the weighted centroid calculation, one can find the location of each light spot more precisely than via simple binary methods. Centroid positions were compared using each method, and an average shift of ~13% was observed.

Because multiple pixels are averaged together to find a light spot centroid, the uncertainty associated with the location of the centroid is lower than that of each pixel. Specifically, the standard deviation of the sum of  $M$  pixel locations is reduced by (K. S. Fu, et al., 1987)  $1 / \sqrt{M}$ .

Unfortunately, not all  $M$  pixels are statistically significant in the centroid calculation. This can be seen by considering the diagram in Fig. 4. When the centroid of the circle is displaced slightly as shown, only the pixels around the circumference of the circle are affected. Therefore, we assert that only these outer pixels are statistically significant in finding the light spot's centroid.

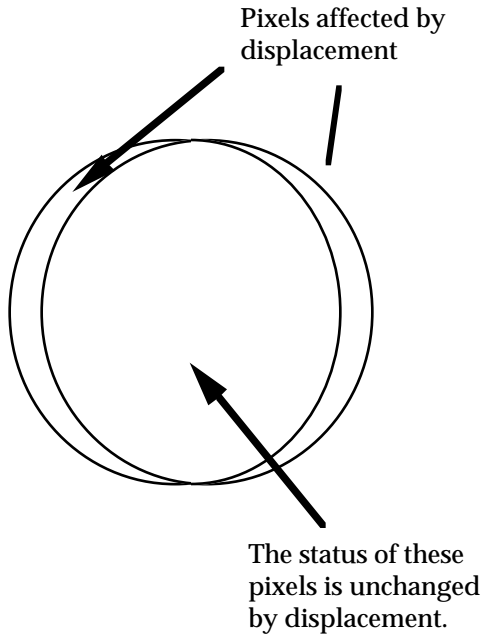


**Fig. 4. Overlapping images of a displaced image feature (circle) are shown. The majority of image pixels contained in the feature are not statistically significant in the calculation of the feature's centroid.**

In the SCOPE calibration jigs, the imaged diameter of each light spot will be  $\sim 12$  pixels. The discrete path length of the circumference (B. K. P. Horn, 1984) of each light spot is therefore  $\sim 48$  pixels. Hence, in the current SCOPE design, the uncertainty of each centroid location will be about  $1/7$  of a pixel.

Once the world coordinates  $(X_i, Y_i, Z_i)$  and the image coordinates  $(R_i, C_i)$  of each light spot have been found, the column vectors  $(L_a, L_b, L_c)$  of the camera model can then be calculated using the relationship majority image pixels contained in the feature are not statistically significant in the calculation of the feature's centroid.

$$\begin{vmatrix} X_1 & Y_1 & Z_1 \\ X_i & Y_i & Z_i \\ X_n & Y_n & Z_n \end{vmatrix} = \begin{vmatrix} 1 & R_1 & C_1 \\ 1 & R_i & C_i \\ 1 & R_n & C_n \end{vmatrix} \begin{vmatrix} L_a & L_b & L_c \end{vmatrix}$$

$$W = PL \quad (2)$$

$W$  is formed with row vectors of the light spots' world coordinates.  $P$  is formed by row vectors of the image coordinates of each light spot centroid. In the previous case, a simple linear model is shown. The row vectors of  $P$  were augmented to permit accurate modeling of the camera's perspective effect and distortions. Experiments were performed with several forms of augmentation. Vectors containing cross terms of the row ( $r$ ) and column ( $c$ ) proved to be most effective, for example,

$$[ 1 \ r \ c \ r^2 \ c^2 \ r^3 \ c^3 \ r^2c \ c^2r \ rc \ r^2c^2 ] \quad (3)$$

Given  $n$  light spots and an augmented vector length of  $d$ , the dimensionality of the elements in Eq. (2) becomes

$$\begin{aligned} W & (n \times 3) \\ P & (n \times d) \\ L & (d \times 3) \end{aligned}$$

Hence, in general,  $P$  is not square, and the Moore-Penrose pseudoinverse (G. Strang, 1980) is useful for finding the camera model:

$$L = (P^T P)^{-1} P^T W \quad (4)$$

The  $P^T P$  matrix inversion has been accomplished via an LU decomposition followed by back substitution (G. Strang, 1980; W. H. Press, B. P. Flanner, S. A. Teukolsky, and W. T. Vetterling, 1988).

Two factors were found to affect the numerical performance of the pseudoinverse. The first was associated with the manipulation of matrices containing coefficients that span many orders of magnitude (P. A. Stark, 1970). By normalizing the image coordinates in  $P$  to the range  $(0, 1)$ , the span of coefficients in  $P^T P$  was reduced from 21 to 8 orders of magnitude.

The second factor effecting numerical performance was the location of the image origin. Early attempts that placed the origin at the center of the image proved to be disastrous when used with a regularly spaced grid of features on the calibration target. These numerical problems occur when the columns of  $P$  become nearly linearly dependent (P. A. Stark, 1970). In an arrangement with symmetric light spots about the origin and with high-order terms, the sign differences of the symmetric centroids vanish, and many of the terms in the  $P$  matrix become nearly identical. This situation leads to intolerable numerical problems even with a second-order camera model. A simple fix of placing the image origin in a corner destroyed the symmetry and eliminated this problem.

**Fig. 5. Intraplane analysis of a camera model.**

## MODEL ANALYSIS

The accuracy of the camera model is evaluated using two methods. The first simply reprocesses the input data. The pixel location of each light spot is fed into the model, and the resulting three-dimensional location is compared to the original location on the calibration plane. This fitting error of the model is used as both a measure of numerical performance of the pseudoinverse and as a measure of the adequacy of the form of the camera model. A simple linear model,

$$[ I r c ] \quad (5)$$

yielded an average fit error of 0.56 pixels. The higher order model in Eq. (3) resulted in a much better average fit of 0.11 pixel. Gray-scale images were generated that describe the fit error across the field of view of the camera (see Fig. 5). The images contain gray blocks located at the position of each original data point. The gray scale of each block is mapped to the corresponding fit error for that data point. Lighter blocks can be seen nearer the periphery, thus indicating that the linear model chosen in this example was not capable of describing the radial distortion of the lens. Any positioning errors of the light spots are also revealed in this analysis.

A second type of analysis on the camera models has also been performed which finds the consistency across multiple models. The consistency of each pixel was mapped to a gray-scale value as an aid in revealing any patterns of errors that may exist in the models. Disagreements between models arose, for example, from misalignments during setup and from data entry errors.

An image produced by this analysis can be seen in Fig. 6. In this example one of the models had been derived using an (intentionally) rotated calibration target. The target had been rotated about the lower left corner. Figure 6 shows darker regions nearer the center of rotation which correspond to a better interplane agreement. The moment arm of the rotation was longest in the upper right corner, as is revealed by the brightest areas shown in Fig. 6.

To generate the image, the camera models were used to generate sets of points along each pixel's sighting vector. The points  $(X_i, Y_i, Z_i)$  were first translated so as to be expressed with respect to their centroid. A best-fit line was then found that passed through the centroid and had a slope of  $(dx/ds, dy/ds, dz/ds)$ , where  $ds$  represents an incremental distance along the line. The vector of slopes was found using

$$\begin{bmatrix} X_1 & Y_1 & Z_1 \\ X_i & Y_i & Z_i \\ X_n & Y_n & Z_n \end{bmatrix} = \begin{bmatrix} S_1 * K_1 \\ S * K_i \\ S_n * K_n \end{bmatrix} \begin{bmatrix} dx & dy & dz \\ ds & ds & ds \end{bmatrix}$$

$$P = SM \quad (6)$$

where

$$\begin{aligned}
 P & (n \times 3) \\
 S & (n \times 1) \\
 M & (1 \times 3) .
 \end{aligned}$$

The elements of  $S$  are scalars formed by the product of  $S_i * K_i$ , where  $S_i$  is the distance from the  $i$ th point to the

centroid and  $K_i$  is  $\pm 1$  depending on the location of the point relative to the centroid. The vector of slopes is found via the pseudo inverse:

$$M = (S^T S)^{-1} S^T P \quad (7)$$

A scalar measure of the model consistency was found by summing the absolute values of an error matrix,  $E$ :

$$E = P - SM \quad (8)$$

The scalar was then mapped to a gray-scale value.

## CONCLUSION

The method of Two Planes for camera calibration has proven to be accurate. Two analysis techniques have been developed which provide a verification of the camera models. The in situ approach to calibration and analysis permits camera calibration to be performed in a hazardous environment without hardware decontamination.

**Fig. 6. Interplane analysis of camera models.**

## REFERENCES

B. L. BURKS, F. W. DEPIERO, J. C. ROWE, C. B. SELLECK, D. L. JACOBOSKI, and R. MARKUS, "Generation of 3-D Surface Maps in Waste Storage Silos Using a Structured Light Source," proceedings of the Space Operations, Applications, and Research Symposium, Houston (1991).

B. L. BURKS, F. W. DEPIERO, M. A. DINKINS, J. C. ROWE, C. B. SELLECK and D. L. JACOBOSKI, "Final Results of the Application of a Structured Light Source for Surface Mapping of the Fernald K-65 Silos," proceedings of the Annual Meeting of the American Nuclear Society, Boston (1992).

K. S. FU, et al., "Robotics: Control, Sensing, Vision and Intelligence," McGraw-Hill, New York (1987).

S. W. HOLLAND, L. ROSSOL, and M. R. WARD, "Computer Vision and Sensor-Based Robotics," Plenum Press, New York (1978)

B. K. P. HORN, *Robot Vision*, MIT Press, Cambridge, Mass., and McGraw-Hill Book Co., New York (1984).

A. ISAGUIRRE, P. PU, and J. SUMMERS, "A New Development in Camera Calibration: Calibrating a Pair of Mobile Cameras," Department of Computer and Information Science, GRASP Laboratory, University of Pennsylvania, Philadelphia (1985).

W. H. PRESS, B. P. FLANNERY, S. A. TEUKOLSKY, and W. T. VETTERLING, "Numerical Recipes in C," Cambridge University Press, Cambridge, New York (1988).

P. A. STARK, "Introduction to Numerical Methods," Macmillan Publishing Co., Inc., New York (1970).

G. STRANG, "Linear Algebra and its Applications," 2nd ed., Academic Press, New York (1980).

G-Q. WEI, and S. DE MA, "Two Plane Camera Calibration: A Unified Model," National Laboratory of Pattern Recognition, Institute of Automation, Chinese Academy of Sciences, Beijing (1991).

**CAMERA CALIBRATION IN A HAZARDOUS ENVIRONMENT  
PERFORMED IN SITU WITH AUTOMATED ANALYSIS AND VERIFICATION\***

Frederick W. DePiero and Reid L. Kress  
Robotics & Process Systems Division  
Oak Ridge National Laboratory  
P.O. Box 2008, Bldg. 7601  
Oak Ridge, Tennessee 37831-6304  
Telephone 615-574-8951  
Facsimile 615-576-2081

The submitted manuscript has been authored by a contractor of the U.S. Government under contract No. DE-AC05-84OR21400. Accordingly, the U.S. Government retains a paid-up nonexclusive, irrevocable, worldwide license to publish or reproduce the published form of this contribution, prepare derivative works, distribute copies to the public, and perform publicly and display publicly, or allow others to do so, for U.S. Government purposes.

To be presented at the  
American Nuclear Society  
Fifth Topical Meeting on  
Robotics & Remote Systems  
Knoxville, Tennessee  
April 26-29, 1993

---

\*Research sponsored by the Office of Technology Development, U.S. Department of Energy, and managed by Martin Marietta Energy Systems, Inc., under contract DE-AC05-84OR21400.